10.1071/EN19100_AC

Environmental Chemistry 2019, 16(8), 599-612

SUPPLEMENTARY MATERIAL

Optimisation of orthophosphate and turbidity removal using an amphoteric chitosan-based flocculant–ferric chloride coagulant system

Henry K. Agbovi[A] and Lee D. Wilson[A,B]

[A]University of Saskatchewan, Department of Chemistry, 110 Science Place, Thorvaldson Building (Room 165), Saskatoon, Saskatchewan, Canada S7N 5C9.

[B]Corresponding author. Email: lee.wilson@usask.ca

1.0 Box-Behnken experimental design

The traditional method of coagulation-flocculation involves changing one factor at a time and requires many experiments, which may be time-consuming, often leading to low optimization efficiency. To address this problem, the design of experiment (DOE) was used to study the effect of variables and their responses using a minimum number of experiments. RSM is a collection of statistical and mathematical methods which are useful for developing, improving, and optimizing processes (Aslan and Cebeci 2007; Aslani et al. 2016; Bezerra et al. 2008). The selection of an adequate experimental design is a key consideration for experimental optimization. The BBD method was employed to obtain the optimum T_i and $P_{i,}$ removal. The BBD is an independent, rotatable quadratic design with no embedded factorial or fractional factorial points, where the variable combinations are at the mid-points of the edges of the variable space and at the center (Usharani and Lakshmanaperumalsamy 2016). The BBD requires fewer treatment combinations than the central composite design, and is less expensive to perform, especially in cases with three or four factors. BBD allows efficient estimation of the first- and second-order coefficients and does not have axial points. Thus, it is certain that all design points fall within a safe operating zone. The BBD approach ensures that not all factors are set at their high levels at the same time. This affords identification of significant effects of interaction for batch studies (Rakić et al. 2014; Usharani and Lakshmanaperumalsamy 2016; Usharani and Muthukumar 2013; Zolgharnein et al. 2013). Preliminary experiments indicate that important variables affecting T_i and $P_{i,}$ removal include ferric chloride dosage, CMC-CTA dosage, pH and settling time (Agbovi and Wilson 2018). These variables were evaluated to optimize T_i and $P_{i,}$ removal. $FeCl_3$ dosage varied between 5 $mg{\cdot}L^{-1}$ and 15 $mg{\cdot}L^{-1}$, CMC-CTA dosage (1 $mg{\cdot}L^{-1}$ to 5 $mg{\cdot}L^{-1}$), pH (2 to 12), and settling time (10 to 60 minutes). In Table 1, the experimental design had four variables (*A, B. C* and *D*), each at three levels, coded as -1, 0 and +1, for low, middle and high values, respectively. Twenty-nine experiments were carried out according to the statistical matrices developed by the RSM, in order to account for variability of the independent variables on T_i and $P_{i,}$ removal. The experimental data was fit using a non-linear regression method with a second order polynomial to identify significant coefficient terms. The application of RSM provides an empirical relationship between the response function and the independent variables. The quadratic response model is based on all linear terms, square terms, and linear interaction terms, according to equation (S1) (Jain et al. 2011).

$$Y = b_{\circ} + \sum b_i x_i + \sum b_{ii} x_{ii}^{\ 2} + \sum b_{ij} x_{ij} \quad \text{(S1)}$$

Here, Y is the predicted response (T_i or P_i, removal efficiency) b_o is the model constant, b_i is the linear coefficient, b_{ii} is the quadratic effect of the input factor x_{ii}, b_{ij} is the linear interaction effect between the input factors x_i and x_j.

The response function coefficients were determined by regression using the experimental data and the Quantum LX Sigmazone DOE regression program. The response functions for turbidity and phosphate removal (%) were approximated by the standard quadratic polynomial equation in eqn (S2), which describes the regression model of the system, including the interaction terms. (Jain et al. 2011)

$$\begin{aligned} Y = {} & b_0 + b_1 A + b_2 B + b_3 C + b_4 D + b_{11} A^2 + b_{12} AB + b_{13} AC + b_{14} AD + b_{22} B^2 + b_{23} BC \\ & + b_{23} BD + b_{33} C^2 + b_{34} CD + b_{33} D^2 \end{aligned} \quad \text{(S2)}$$

Here, Y is the predicted response, T_i or P_i removal (%); A, B, C and D are the coded levels of the independent variables: CMC-CTA dose (mg/L), $FeCl_3$ (mg/L) dose, pH and settling time (minutes), respectively. The regression coefficient, b_0 denotes the intercept term; b_1, b_2, b_3 and b_4 represent the linear coefficients; b_{12}, b_{13}, b_{14}, b_{23}, b_{24}, b_{34} represent the interaction coefficients and b_{11}, b_{22}, b_{33} and b_{44} denote the quadratic coefficients. Analysis of variance (ANOVA) was employed to perform diagnostic tests on the adequacy of the proposed model. The ANOVA test estimates the suitability of the response functions and the significance of the effects for the independent variables.

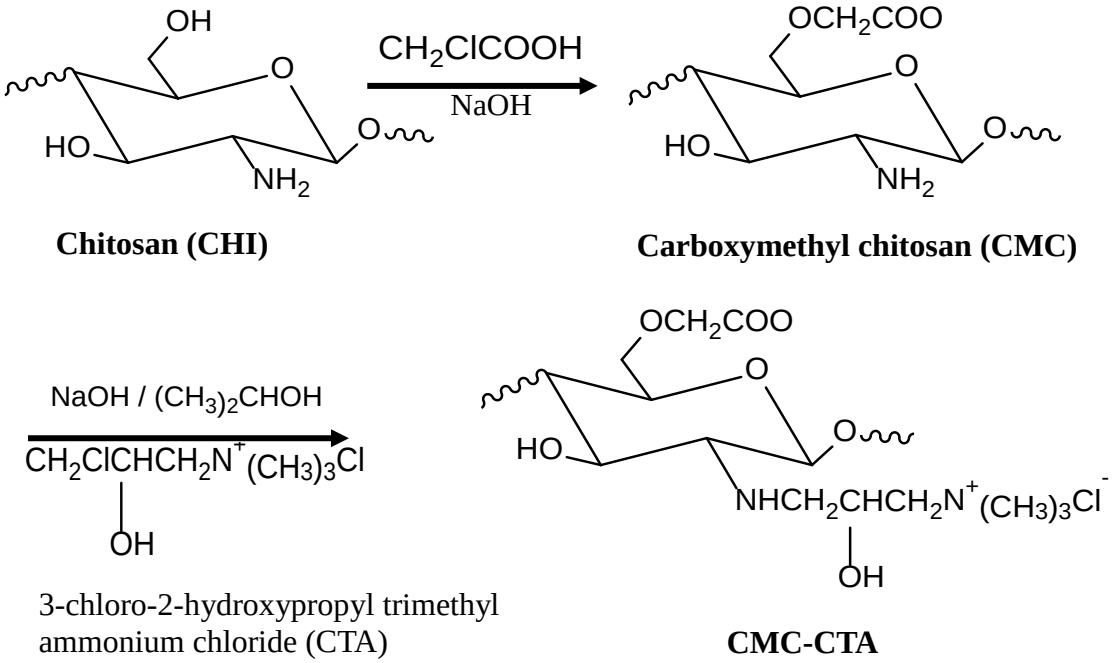

Chitosan (CHI)

Carboxymethyl chitosan (CMC)

3-chloro-2-hydroxypropyl trimethyl ammonium chloride (CTA)

CMC-CTA

Scheme S1: Synthetic route of carboxymethyl chitosan (CMC) and 3-chloro-2-hydroxypropyl trimethylammonium chloride grafted onto CMC (CTA-CMC).

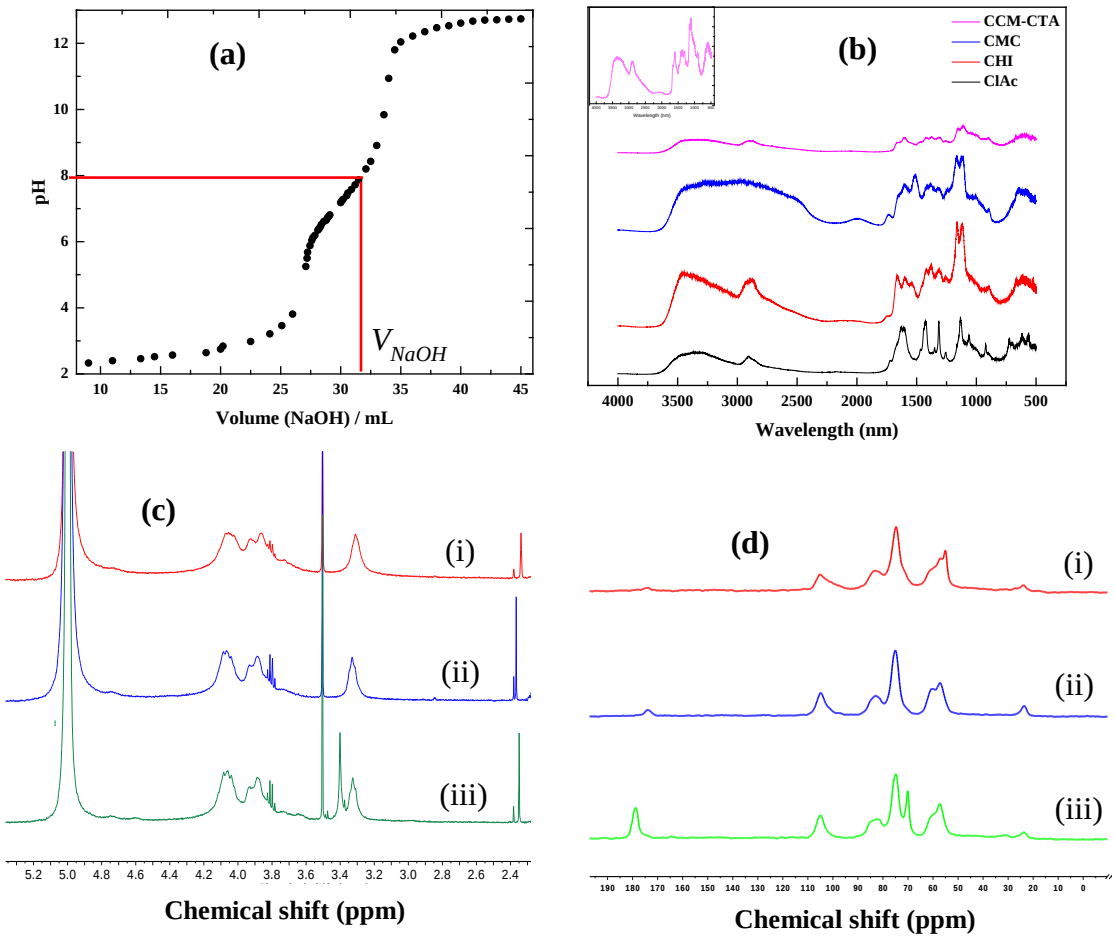

Figure S1: (a) Titration curve for estimation of the DS for CMC, where V_{NaOH} denotes the titrant volume of NaOH at the equivalent point (b) FT-IR spectra of chloroacetic acid (ClAc), Chitosan (CHI), CMC and CMC-CTA. The insert is an IR spectrum of CMC-CTA. (c) ^{1}H-NMR spectra of chitosan (i), carboxymethyl chitosan, CMC (ii) and CMC-CTA (iii). (d) ^{13}C-NMR of chitosan (i), carboxymethyl chitosan, CMC (ii) and CMC-CTA (iii).

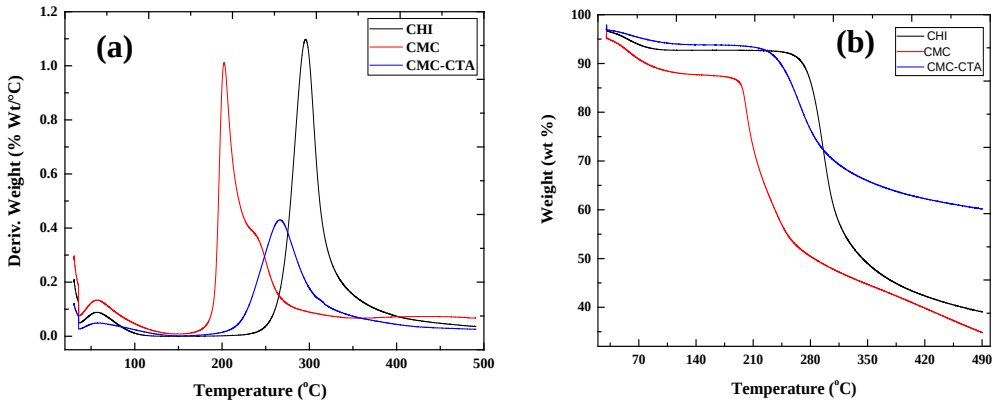

Figure S2: TGA profile of chitosan, carboxymethyl chitosan (CMC) and CMC-CTA: (a) First derivative of weight loss (wt/°C) against temperature, and (b) weight loss with temperature.

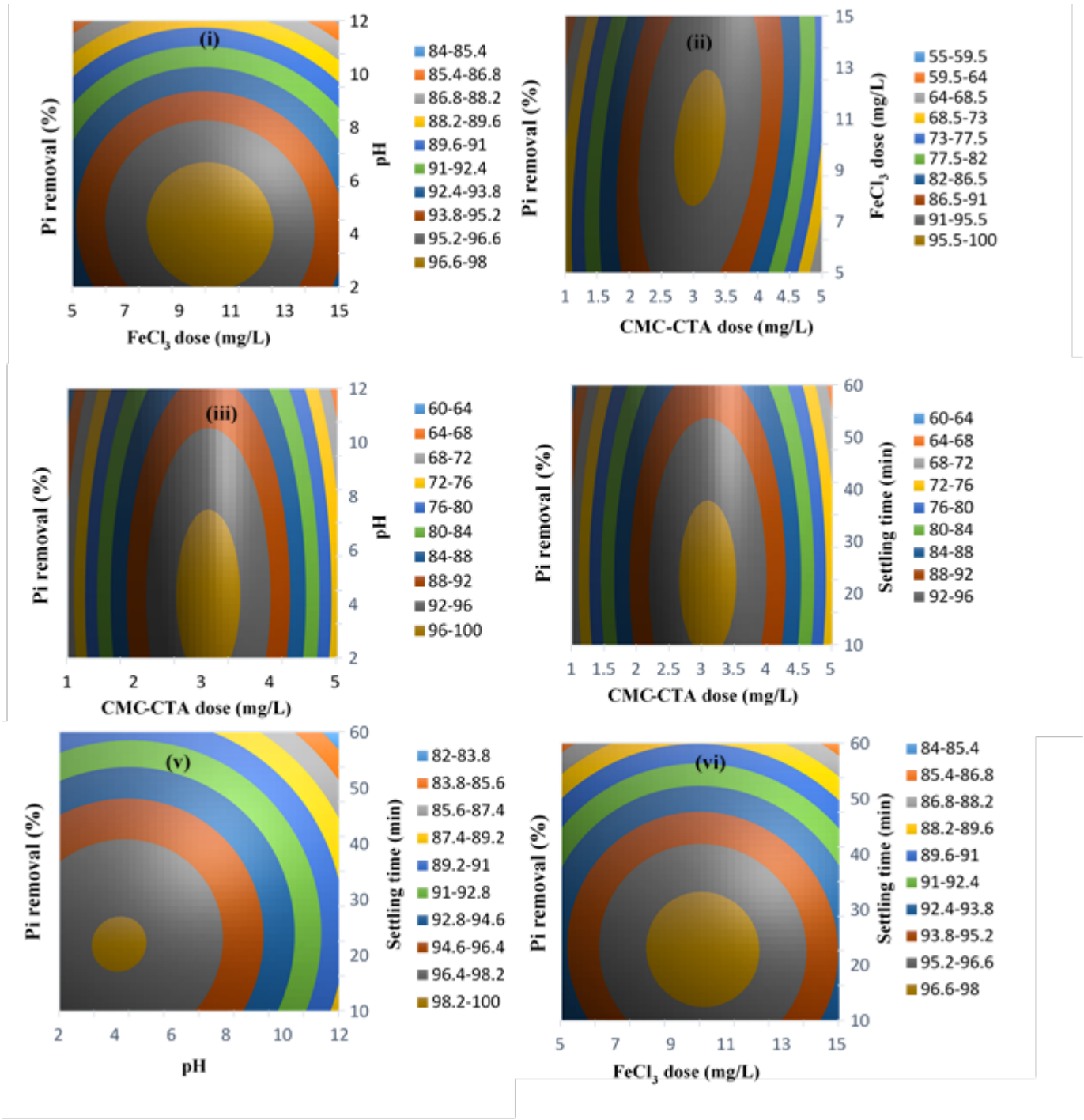

Figure S3: Two-dimensional Box-Behnken contour plots of phosphate removal efficiency as a function of (i) pH and $FeCl_3$; (ii) CMC-CTA dose and $FeCl_3$ dose; (iii) CMC-CTA dose and pH; (iv) CMC-CTA dose and setting time; (v) pH and settling time; and (vi) $FeCl_3$ dosage and settling time.

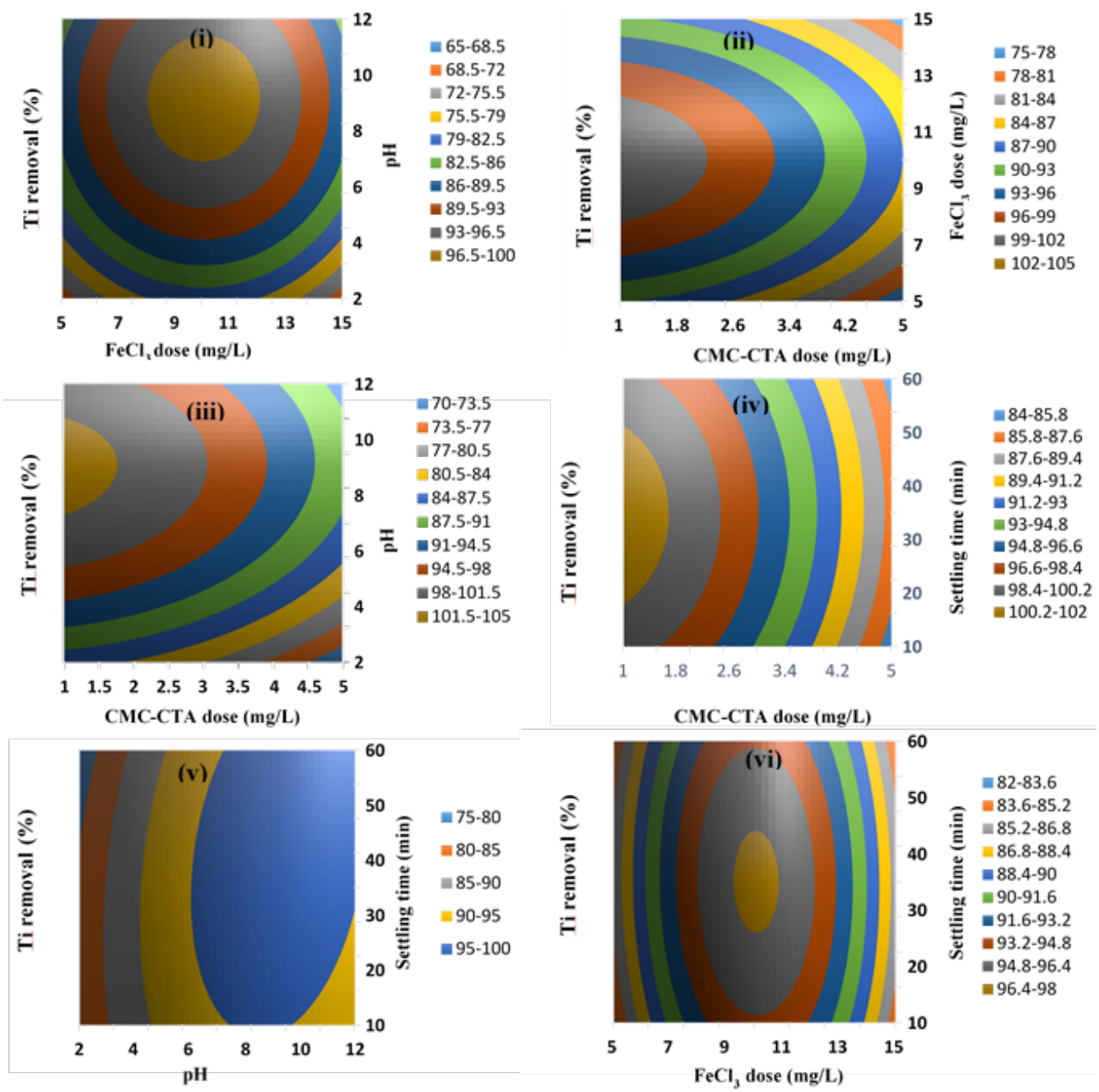

Figure S4: Two-dimensional Box-Behnken contour plots of T_i removal efficiency as a function of (i) pH and $FeCl_3$; (ii) CMC-CTA dose and $FeCl_3$ dose; (iii) CMC-CTA dose and pH; (iv CMC-CTA dose and setting time.

Table S1: Comparison of the removal of phosphate in water and wastewater using different coagulant-flocculant systems.

Water Source	Flocculant	Optimum Dosage (mg/L)	Optimum pH	Efficiency (%)	Reference
Synthetic wastewater	Fe(III)-CMC-CTA	10, 3.0	6.5	96.4	This work
Synthetic wastewater	Chitosan	20	6.2 - 7.0	78 ± 0.1	(Agbovi et al. 2017)
Synthetic wastewater	Chitosan + Alum	49	5.8 - 7.0	88 ± 0.8	(Agbovi et al. 2017)
Struvite	Chitosan and Alginate	10, 20	N/A	80	(Latifian et al. 2014)
Synthetic wastewater	Chitosan	N/A	7.5 - 7.9	60	(Fierro et al. 2008)
Synthetic wastewater	Chitosan	N/A	4	30	(Filipkowska et al. 2014)
Municipal wastewater	Chitosan	60	9.5	89	(Dunets and Zheng 2015)
Synthetic wastewater	Chitosan + PAC	67.9; 20.05	7.5	99.4	(Li et al. 2019)
Synthetic wastewater	Zirconium ion modified chitosan	50	4	60.6	(Liu and Zhang 2015)
Agricultural wastewater	HMW Chitosan	12	7.2	99.1	(Chung et al. 2005)
Municipal wastewater	Chitosan	10	7	98	(Turunen et al. 2019)
Synthetic wastewater	Chitosan	7	4	59.5	(Agbovi and Wilson 2018)
Synthetic wastewater	CMC-CTA	5	6.5	70.5	(Agbovi and Wilson 2018)
Synthetic wastewater	CMC	8	6.5	29.8	(Agbovi and Wilson 2018)

Table S1 Continued

Water Source	Flocculant	Optimum Dosage (mg/L)	Optimum pH	Efficiency (%)	Reference
Synthetic wastewater	$FeCl_3$ + chitosan	7.5 + 7	6.5	88.8	(Agbovi and Wilson 2018)
Synthetic wastewater	$FeCl_3$ + CMC	7.5 + 9	6.5	68.8	(Agbovi and Wilson 2018)
Synthetic wastewater	$CaCl_2$ + CS-g-PAD	6	10	98.8	(Sun et al. 2016)
Secondary effluent	Chitosan	5.5	5	80	(Rojsitthisak et al. 2017)
Activated sludge effluent discharge	Ferrous chloride	13	N/A	80	(An et al. 2014)
Synthetic wastewater	Ferric chloride	80	7.2	82	(Yang et al. 2010)
Secondary effluent wastewater	Alum	10	5.7−5.9	92	(Banu et al. 2007)
Synthetic wastewater	Polydiallyldimethyl-ammonium chloride	0.5	8	59	(Chen and Luan 2010)

References

Agbovi, H.K., Wilson, L.D., 2018. Design of amphoteric chitosan flocculants for phosphate and turbidity removal in wastewater. *Carbohydr. Polym.* **189**, 360–370. https://doi.org/10.1016/J.CARBPOL.2018.02.024

Agbovi, H.K., Wilson, L.D., Tabil, L.G., 2017. Biopolymer Flocculants and Oat Hull Biomass To Aid the Removal of Orthophosphate in Wastewater Treatment. *Ind. Eng. Chem. Res.* **56**, 37–46. https://doi.org/10.1021/acs.iecr.6b04092

An, J.-S., Back, Y.-J., Kim, K.-C., Cha, R., Jeong, T.-Y., Chung, H.-K., 2014. Optimization for the removal of orthophosphate from aqueous solution by chemical precipitation using ferrous chloride. *Environ. Technol.* **35**, 1668–1675. https://doi.org/10.1080/09593330.2013.879495

Aslan, N., Cebeci, Y., 2007. Application of Box – Behnken design and response surface methodology for modeling of some Turkish coals. *Fuel* **86**, 90–97. https://doi.org/10.1016/j.fuel.2006.06.010

Aslani, H., Nabizadeh, R., Nasseri, S., Mesdaghinia, A., Alimohammadi, M., Mahvi, A.H., Rastkari, N., Nazmara, S., 2016. Application of response surface methodology for modeling and optimization of trichloroacetic acid and turbidity removal using potassium ferrate(VI). *Desalin. Water Treat.* **3994**, 1–12. https://doi.org/10.1080/19443994.2016.1147380

Banu, R.J., Do, K.U., Yeom, I.T., 2007. Phosphorus removal in low alkalinity secondary effluent using alum. *Int. J. Environ. Sci. Technol.* **5**, 93–98. https://doi.org/10.1007/BF03326001

Bezerra, M.A., Santelli, R.E., Oliveira, E.P., Villar, L.S., Escaleira, L.A., 2008. Response surface methodology (RSM) as a tool for optimization in analytical chemistry. *Talanta* **76**, 965–977. https://doi.org/10.1016/j.talanta.2008.05.019

Chen, J., Luan, Z., 2010. Enhancing Phosphate Removal by Coagulation Using Polyelectrolytes and Red Mud. *Fresenius Environ. Bull.* **19**, 2200–2204.

Chung, Y.C., Li, Y.H., Chen, C.C., 2005. Pollutant removal from aquaculture wastewater using the biopolymer chitosan at different molecular weights. *J. Environ. Sci. Heal. - Part A Toxic/Hazardous Subst. Environ. Eng.* **40**, 1775–1790. https://doi.org/10.1081/ESE-200068058

Dunets, C.S., Zheng, Y., 2015. Combined Precipitation / Flocculation Method for Nutrient Recovery from Greenhouse Wastewater. *Hortscience* **50**, 921–926.

Fierro, S., del Pilar Sánchez-Saavedra, M., Copalcúa, C., 2008. Nitrate and phosphate removal by chitosan immobilized Scenedesmus. *Bioresour. Technol.* **99**, 1274–1279. https://doi.org/10.1016/j.biortech.2007.02.043

Filipkowska, U., Jóźwiak, T., Szymczyk, P., 2014. Application of Cross-Linked Chitosan for Phosphate Removal From Aqueous Solutions. *Prog. Chem. Appl. Chitin its Deriv.* **19**, 5–14. https://doi.org/10.15259/PCACD.19.01

Jain, M., Garg, V.K., Kadirvelu, K., 2011. Investigation of Cr(VI) adsorption onto chemically treated Helianthus annuus: Optimization using Response Surface Methodology. *Bioresour. Technol.* **102**, 600–605. https://doi.org/10.1016/j.biortech.2010.08.001

Latifian, M., Liu, J., Mattiasson, B., 2014. Recovery of struvite via coagulation and flocculation using natural compounds. *Environ. Technol.* **35**, 2289–2295. https://doi.org/10.1080/09593330.2014.902110

Li, Y., Li, L., Yasser Farouk, R., Wang, Y., 2019. Optimization of Polyaluminum Chloride-Chitosan Flocculant for Treating Pig Biogas Slurry Using the Box–Behnken Response Surface Method. *Int. J. Environ. Res. Public Health* **16**, 996. https://doi.org/10.3390/ijerph16060996

Liu, X., Zhang, L., 2015. Removal of phosphate anions using the modified chitosan beads: Adsorption kinetic, isotherm and mechanism studies. *Powder Technol.* **277**, 112–119. https://doi.org/10.1016/j.powtec.2015.02.055

Rakić, T., Kasagić-Vujanović, I., Jovanović, M., Jančić-Stojanović, B., Ivanović, D., 2014. Comparison of Full Factorial Design, Central Composite Design, and Box-Behnken Design in Chromatographic Method Development for the Determination of Fluconazole and Its Impurities. *Anal. Lett.* **47**, 1334–1347. https://doi.org/10.1080/00032719.2013.867503

Rojsitthisak, P., Burut-Archanai, S., Pothipongsa, A., Powtongsook, S., 2017. Repeated phosphate removal from recirculating aquaculture system using cyanobacterium remediation and chitosan flocculation. *Water Environ. J.* **31**, 598–602. https://doi.org/10.1111/wej.12288

Sun, Y., Ren, M., Zhu, C., Xu, Y., Zheng, H., Xiao, X., Wu, H., Xia, T., You, Z., 2016. UV-Initiated Graft Copolymerization of Cationic Chitosan-Based Flocculants for Treatment of Zinc Phosphate-Contaminated Wastewater. *Ind. Eng. Chem. Res.* **55**, 10025–10035. https://doi.org/10.1021/acs.iecr.6b02855

Turunen, J., Karppinen, A., Ihme, R., 2019. Effectiveness of biopolymer coagulants in agricultural wastewater treatment at two contrasting levels of pollution. *SN Appl. Sci.* **1**, 1–9. https://doi.org/10.1007/s42452-019-0225-x

Usharani, K., Lakshmanaperumalsamy, P., 2016. Box-behnken experimental design mediated optimization of aqueous methylparathion biodegradation by Pseudomonas aeruginosa MPD strain. *J. Microbiol. Biotechnol. Food Sci.* **05**, 534–547. https://doi.org/10.15414/jmbfs.2016.5.6.534-547

Usharani, K., Muthukumar, M., 2013. Optimization of aqueous methylparathion biodegradation by Fusarium sp in batch scale process using response surface methodology. *Int. J. Environ. Sci. Technol.* **10**, 591–606. https://doi.org/10.1007/s13762-012-0144-5

Yang, K., Li, Z., Zhang, H., Qian, J., Chen, G., 2010. Municipal wastewater phosphorus removal by coagulation. *Environ. Technol.* **31**, 601–609. https://doi.org/10.1080/09593330903573223

Zolgharnein, J., Shahmoradi, A., Ghasemi, J.B., 2013. Comparative Study of Box-BehnKen, central composite, and Doehlert matrix for multvariate optimization of Ph (II) adsorption onto Robinian tree leaves. *J. Chemom.* **27**, 12–20.